water

MDPI

Article

Transport Behavior of RB5 Dye in Alluvial Soil in the Northeast of Brazil

Adriana Thays Araújo Alves [1], Artur Paiva Coutinho [1,*], Vitor Hugo de Oliveira Barros [1], Laurent Lassabatere [2], Severino Martins dos Santos Neto [1], José Romualdo de Sousa Lima [3] and Antonio Celso Dantas Antonino [4]

1 Centre of Agreste Academic, Department of Civil Engineering, Federal University of Pernambuco, Caruaru 55014-900, Brazil; adrianathaaraujo@gmail.com (A.T.A.A.); vitor_barros1@outlook.com (V.H.d.O.B.); martinsdsn@gmail.com (S.M.d.S.N.)
2 UMR5023 Ecologie des Hydrosystèmes Naturels et Anthropisés, Univ Lyon, Université Claude Bernard Lyon 1, CNRS, ENTPE, F-69518 Vaulx-en-Velin, France; laurent.lassabatere@entpe.fr
3 Department of Agronomy, Federal University of Agreste of Pernambuco, Garanhuns 55292-270, Brazil; romualdo.lima@ufape.edu.br
4 Centre for Technology and Geosciences, Department of Nuclear Energy, Federal University of Pernambuco, Recife 50740-545, Brazil; antonio.antonino@ufpe.br
* Correspondence: arthur.coutinho@yahoo.com.br or arthur.coutinho@ufpe.br; Tel.: +55-81985453356

Abstract: The textile industry generates a large volume of chemically diversified effluents containing, among other compounds, dyes. Untreated wastes are contaminants to surface water, soil, and groundwater. In this aspect, various studies have explored the issue of contamination of alluvial soils in the Alto Capibaribe region, northeast of Brazil, due to local textile activity. This region, inserted into the Brazilian semiarid region, suffers from water scarcity, and there is a need for rural communities to use alluvial formations for water supply. The simulation of solute transport is a fundamental tool for understanding the environmental performance and risks associated with contamination by textile dyes. Transport parameters that directly influence pollutant dynamics in sedimentary environments are characterized. This study evaluated the retention and mobility of the dye Remazol Black 5 (RB5) in two superficial layers of alluvial soil from Alto Capibaribe to obtain transport parameters. In the laboratory, tests of mobility in soil columns with RB5 dye (concentration of the 25 mg L^{-1}) and KBr tracer (concentration of the 35.7 g L^{-1}) solutions were conducted. The CDE and two-region models were used to model the KBr experimental transport data, and the two-site model was used to model the RB5 experimental transport data. Physical non-equilibrium was found in the soils for KBr transport, and the two-region model adequately modeled the experimental breakthrough curves (BTCs). For the transport of RB5, the results showed a chemical non-equilibrium, and the two-site model was adequate to model the experimental BTCs. The results indicate that the surface layer is most responsible for the retention of RB5, where the RB5 solution was less mobile than in the lower layer. Both layers showed low retention and high mobility for RB5, indicating that the RB5 dye in the region may contaminate groundwater.

Keywords: alluvial aquifers; breakthrough curve; mobility

Citation: Alves, A.T.A.; Coutinho, A.P.; de Oliveira Barros, V.H.; Lassabatere, L.; dos Santos Neto, S.M.; de Sousa Lima, J.R.; Antonino, A.C.D. Transport Behavior of RB5 Dye in Alluvial Soil in the Northeast of Brazil. *Water* **2022**, *14*, 1000. https://doi.org/10.3390/w14071000

Academic Editor: Anna Barra Caracciolo

Received: 19 January 2022
Accepted: 17 March 2022
Published: 22 March 2022

1. Introduction

In textile processing, dyeing is fundamental for the commercial success of associated products, which explains the diversity of available dyes. Dyeing is the process of imparting colors to a textile material through a stain [1] by migrating the dye molecule into the fiber [2]. It is estimated that 10–15% of the used dyes would be lost in the effluent during the dyeing process [3,4].

Because of the complex aromatic molecular structure, dyes are resistant to degradation processes, causing bioaccumulation in living organisms [5]. Among the reported harmful effects of these compounds are carcinogenic potential and interfering with the photosynthetic activity of some aquatic plants [6,7].

Kharat [8] reported cases where the indiscriminate discharge of textile effluents affected soil and groundwater quality. According to Smaranda et al. [9], some synthetic dyes are soil pollutants of concern due to their toxic nature and adverse effects on life forms. According to Rehman et al. [10], especially around textile processing units, a large concentration of azo dyes can accumulate in surface soils.

Azo dyes are characterized by one or more nitrogen to nitrogen double bonds (–N=N–) and are widely used in the dyeing industry [7]. It is estimated that about half of the world's dye industry production belongs to this class [6]. As a result, large quantities of these compounds are discharged into the environment, causing enormous ecological problems [11]. Remazol Black 5 (RB5) is an azo dye considered popular in the textile industry [12–15]. A large amount of RB5 is discharged in the watercourses of developing countries [15].

In the state of Pernambuco, northeast Brazil, the textile industry has recognized economic relevance. Located in the mesoregion Agreste of Pernambuco, the "Textile Center" is an essential productive arrangement with high national significance. Despite robust industrialization, the Agreste of Pernambuco is affected by water scarcity, marked by low rainfall, high evapotranspiration rates, and intermittent rivers with flow only in the rainy season. Due to water scarcity, many rural communities in this region use underground reservoirs, such as alluvial deposits, by digging wells in the dry riverbed [16], possibly because of the intermittence mentioned, as occurs in the highest portion of the Capibaribe River, called the Alto Capibaribe region. These geological formations often occupy the beds of temporary rivers in the northeastern semiarid region [17] and are an essential water supply source. From a compositional point of view, the alluvial deposits in the Alto do Capibaribe region are highly heterogeneous geological formations, with the contrast of hydrodynamic properties that enable the establishment of preferential flows and regions for the retention of pollutants [18].

As far as is known, studies on RB5 found in the specialized literature focus on analyzing techniques for removing the dye from the aqueous solution. For example, Febrianto et al. [19] identified the ability of different materials to remove RB5 from textile wastewater. The authors concluded that film composite-based membranes based on polyetherimide polymer (PEI-TFC) could separate textile dye wastewater with 92% rejection. Zhu et al. [20], in turn, found that thin-film nanocomposite (TFN) membranes containing poly(sodium 4-styrene-sulfonate) (PSS) modified ZIF-8 (mZIF) in the polyamide (PA) layer, or simply mZIF-functionalized PA membranes, retain >99.0% of the RB5. However, none of these studies investigated the transfer of RB5 in the vadose zone or groundwater, whereas large areas, such as the Capibaribe River watershed, may be affected by this pollutant.

Alves et al. [12] and Alexandre et al. [17] assessed the local textile industry's environmental contamination in the Alto Capibaribe region. The authors examined the sorption, respectively, of RB5 and Direct Black 22 dyes in alluvial deposits by kinetic and isotherm sorption experiments. According to Alexandre et al. [17], alluvial soils are the destination of indiscriminate wastewater disposal by the region's textile industry. This problem gains even more relevance when one considers the high mobility of anionic dye in alluvial soil, especially for deeper layers [12,17].

In scientific literature, batch and column experiments, jointly or separately, are widely used to understand the transport and fate of dyes in the environment [3,9,12,17,21–23]. The disadvantage of batch experiments is the high liquid–solid ratio. In contrast, miscible displacement experiments, the method employed in this study, are closer to the actual situation in describing the solute transport process in the soil [24], being able to simulate, for example, the heterogeneity of the layers and compaction of the soil. The fundamental transport parameters in the column experiment can predict contaminant plume in natural porous media [25].

The modeling of water and solute transport in the soil is an important tool for finding ways to reduce contamination in surface and groundwater [26]. The convection–dispersion equation (CDE) is broadly used to describe solute transport processes in porous media.

However, many laboratory and field experiments have demonstrated the presence of nonequilibrium flow and transport conditions in soils [27]. In these cases, the CDE model may not adequately describe the transport conditions and breakthrough curves (BTCs) characterized by tailing. Chemical non-equilibrium is a kinetic process attributed to a slow sorption reaction at the solid–solution interface or a slow diffusion to sorption sites [28]. For physical nonequilibrium, the two-region nonequilibrium model [29] is frequently cited in the scientific literature to describe solute transport and considers, contrary to CDE, the existence of a stagnant region in porous media and solute exchange between flowing and stagnant regions [30]. For chemical non-equilibrium, the two-site nonequilibrium considers different adsorption sites: type 1 (equilibrium) and type 2 (first-order kinetics) [27,31,32].

In the study of pollutant transport in the soil, it is common to use tracers, i.e., chemicals easy to measure and that do not interact with soil, in order to trace water [26,33,34]. One of the most used tracers is bromide (Br-) at several scales in laboratory conditions [33–39] and in the field [26]. In view of what has been exposed here, the objective of the present study was to evaluate the mobility of RB5 dye and understand the dynamics of this solute transfer process in an alluvial deposit typical of the Alto Capibaribe River (Agreste of Pernambuco, Brazil). RB5 dye was chosen since it is quite common in stormwater in the textile industry. In addition, this solute has rarely been studied, and its behavior in soils is scarcely known. The column experiments aim to investigate the transfer of RB5 and its sensitivity to physical and chemical non-equilibria, with the final aim of understanding the risk associated with this dye in alluvial soil in northeast Brazil.

2. Materials and Methods

2.1. Study Area

The studies were conducted in the Alto Capibaribe region, which embraces the highest portion of the Capibaribe River watershed in the state of Pernambuco, Brazil. The soil samples were collected in the dry riverbed in the portion between the municipalities of Santa Cruz do Capibaribe and Brejo da Madre de Deus (7°56′57.6″ S and 36°17′57.2″ W) (Figure 1). In particular, in the dry bed of the Capibaribe River, a trench was dug (12.00 m × 5.00 m × 2.00 m) to investigate the sedimentary architecture of the deposit, in which 4 main layers were identified [18]. Soil samples were collected from the first two soil layers, with Layer 1 (CM1) presenting a maximum thickness of 52 cm and Layer 2 (CM2) dimensions ranging between 17 and 81 cm. Around 50 kg of soil was collected from each layer for laboratory experiments and analyses [18]. The soil parameters were obtained by analyses of the soils already available from [12] and are tabulated in Table 1.

Table 1. Main characteristics of the analyzed soils (from [12,18]).

Layer	Sand (%)	Silt (%)	Clay (%)	Classification	pH in Water	ZPC	OM (%)	OC (%)	CEC (cmolc dm^{-3})
CM1	79.395 ± 0.35	15.71 ± 0.20	4.895 ± 0.35	Loamy sand	8.26 ± 0.28	5.50 ± 0.20	2.17	1.26	7.4
CM2	95.48 ± 0.40	4.205 ± 0.35	0.315 ± 0.29	Sand	6.01 ± 0.35	6.00 ± 0.35	1.67	0.97	3.3

±standard deviation.

2.2. Chemicals, Solutions, and Experimental Setup

Remazol Black 5 (RB5) is an anionic dye widely used by the textile industry of Agreste of Pernambuco. RB5 was obtained from Sigma Aldrich Chemie GmbH (Sao Paulo, Brazil) with a dye content of 55%. The main features of the RB5 dye are presented in Table 2.

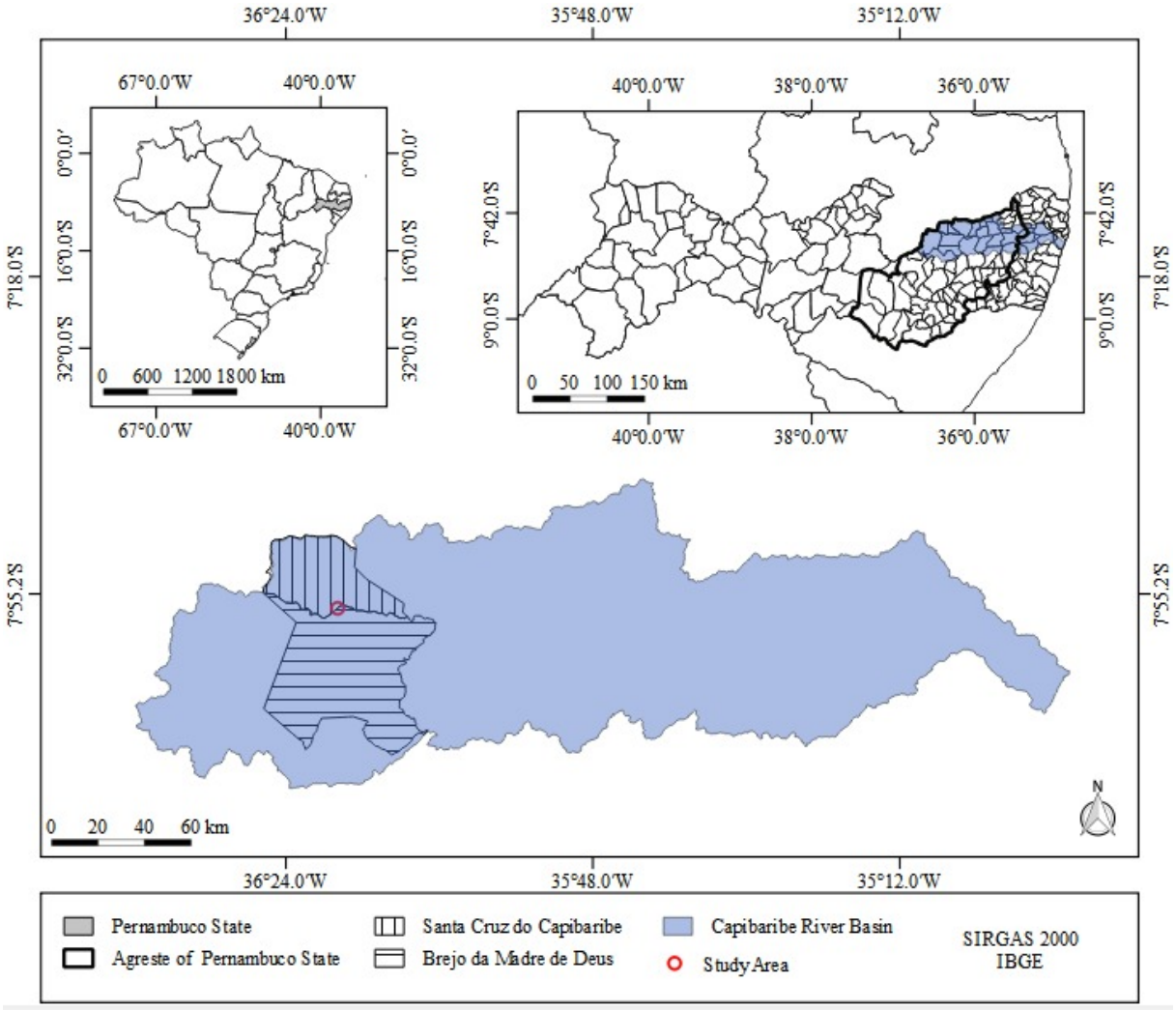

Figure 1. Location of the study area.

Table 2. Characteristics of Remazol Black B-RB5 (adapted from [40]).

Dye	C.I. Reactive Black 5
Molecular formula	$C_{26}H_{21}N_5Na_4O_{19}S_6$
Molecular weight (g.mol^{-1})	991,8
λ_{max} (nm)	597
Classification	Azo, anionic
Chemical structure	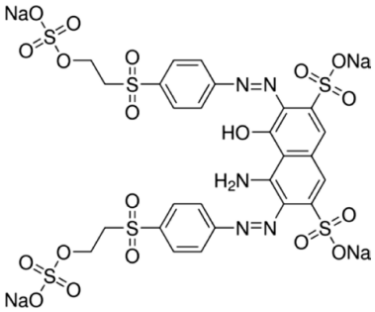
Brand	Sigma-Aldrich
Dye content	≥50%
CAS-No	17095-24-8

Table 2. *Cont.*

EC-No	241-164-5
Component	Tetrasodium 4-amino-5-hydroxy-3,6-bis[[4-[[2-(sulphonatooxy) ethyl] sulphonyl] phenyl] azo] naphthalene-2,7-disulphonate
Classification	Resp. Sens. Category 1, H334; Skin Sens. Category 1, H317

Bromide in the form of KBr, obtained from SigmaAldrich Chemie GmbH (Sao Paulo, Brazil) at a concentration of 35.70 g L^{-1} (0.3 mol L^{-1}) was used as a non-reactive tracer in the column experiments to determine physical transport parameters. The concentration of RB5 dye was 25 mg L^{-1}, and the preparation of solutions was performed according to the procedure described in [12].

The experimental setups used for the conservative tracer (KBr) and RB5 transport experiments are shown in Figure 2. The studies were conducted using a transparent acrylic cylinder column (internal diameter of 2.6 cm and length of 30 cm) at a constant flow rate under saturated flow conditions. The columns were filled with soils and compacted homogeneously until reaching a soil bulk density equal to the field density (1.52 g cm^{-3} for CM1 and 1.63 g cm^{-3} for CM2).

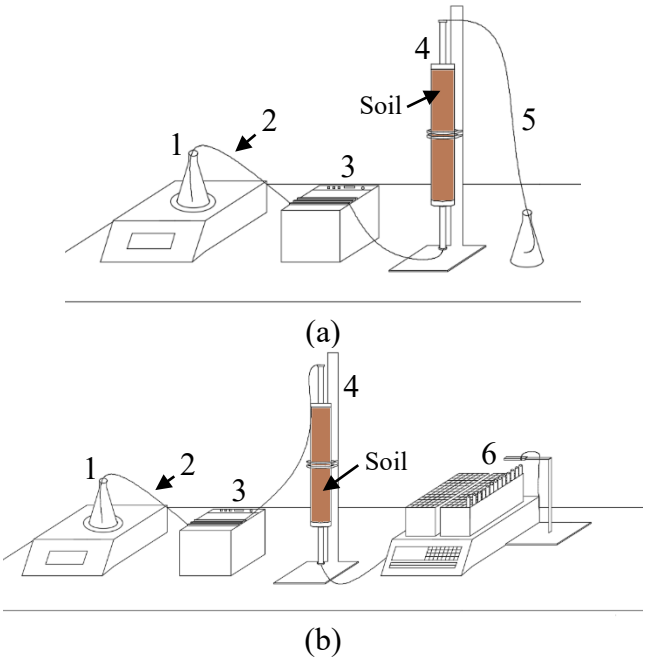

1. digital scales;
2. flexible silicone capillary tube;
3. peristaltic pump;
4. acrylic cylinder column;
5. effluent collector;
6. effluent collector (fraction).

Figure 2. Schematic design of the fixed bed column used for saturation of the soil column in upward flow mode (**a**) and displacement of KBr and RB5 solutions in downward flow (**b**).

The soil column was saturated in an upward flow with $CaCl_2$ solution (calcium chloride), purchased from Vetec Química Fina Ltd.a (Rio de Janeiro, Brazil) with a concentration of 1.20 g L^{-1} (0.01 mol L^{-1}). The volume used to saturate the column corresponded to 1 pore volume. After the column was saturated, we injected one pore volume of the KBr solution at a concentration of 35.70 g L^{-1} (0.3 mol L^{-1}) and a flow rate of 0.32 mL min^{-1}, followed by the injection of $CaCl_2$ solution to leach the KBr from the soil column. The effluent solutions from the column were collected using an automatic fraction collector. The electrical conductivity of the leachates was determined with a DIGIMED DM-31 conductivity meter.

Afterward, one pore volume of the RB5 solution (25 mg L^{-1}) was introduced into the columns in a downward flow. The injection of $CaCl_2$ solution followed this step to leach RB5 from the soil column. The effluent solutions from the column were collected using an automatic fraction collector. Finally, the absorbance was taken at 597 nm in a

spectrophotometer (Thermo Scientific GENESYS 30 Visible Spectrophotometer) to determine the concentrations. The evolution of the relative concentration C/C_0 was plotted against the number of pore volumes (V/V_0) to determine the BTCs. The experiments were performed in triplicate, and the average breakthrough curves (BTCs) were plotted.

2.3. Transport Models

Flow in the vadose zone is generally in the vertical direction [41]. For several practical applications, the transport of solutes in soil can be modeled using the general convection-dispersion equation (CDE). Using the dimensionless parameters listed in Table 3 adapted from Toride et al. [42], the CDE model can be written in dimensionless form as:

$$R\frac{\partial C_r}{\partial T} = \frac{1}{Pe}\frac{\partial^2 C_r}{\partial Z^2} - \frac{\partial C_r}{\partial Z} - \mu^E C_r + \gamma^E(Z) \quad (1)$$

where R is the retardation factor; C_r is the relative concentration; Pe is the Peclet number; μ^E is the first-order decay coefficient; γ^E is the zero-order production coefficient for equilibrium transport; Z is the dimensionless coordinate; T is the dimensionless time. Chemical equilibrium was assumed, and sorption was linear. When there is no interaction between soil and solute, K_d equals 0 and, consequently, R equals 1.

Table 3. Dimensionless parameters for the CDE, two-site, and two-region models (adapted from [42]).

Parameters	Expressions		
	CDE	**Two-Site Model**	**Two-Region Model**
T	$\frac{vt}{L}$	$\frac{vt}{L}$	$\frac{vt}{L}$
Z	$\frac{x}{L}$	$\frac{x}{L}$	$\frac{x}{L}$
Pe	$\frac{vL}{D}$	$\frac{vL}{D}$	$\frac{v_m L}{D_m} = \frac{vL}{D}$
R	$1+\frac{\rho_d K_d}{\theta}$	$1+\frac{\rho_d K_d}{\theta}$	$1+\frac{\rho_d K_d}{\theta}$
β	-	$\frac{\theta+\rho_d f K_d}{\theta+\rho_d K_d}$	$\frac{\theta_m+\rho_d f K_d}{\theta+\rho_d K_d}$
ω	-	$\frac{\alpha (1-\beta)RL}{v}$	$\frac{\alpha L}{\theta v}$
C	$\frac{c}{c_0}$	-	-
C_1	-	$\frac{c}{c_0}$	$\frac{c_m}{c_0}$
C_2	-	$\frac{s_k}{(1-f)K_d c_0}$	$\frac{c_{im}}{c_0}$
μ^E	$\frac{L(\theta\mu_l+\rho_d K_d \mu_s)}{\theta v}$	-	-
μ_1	-	$\frac{L(\theta\mu_l+f\rho_d K_d \mu_{s,e})}{\theta v}$	$\frac{L(\theta_m \mu_{l,m}+f\rho_d K_d \mu_{s,m})}{\theta v}$
μ_2	-	$\frac{L(1-f)\rho_d K_d \mu_{s,k}}{\theta v}$	$\frac{L(\theta_{im}\mu_{l,im}+(1-f)\rho_d K_d \mu_{s,im})}{\theta v}$
γ^E	$\frac{L(\theta\gamma_l+\rho_d\gamma_s)}{\theta v C_0}$	-	-
γ_1	-	$\frac{L(\theta\gamma_l+f\rho_d\gamma_{s,e})}{\theta v c_0}$	$\frac{L(\theta_m\gamma_{l,m}+f\rho_d\gamma_{s,m})}{\theta v c_0}$
γ_2	-	$\frac{L(1-f)\rho_d\gamma_{s,k}}{\theta v c_0}$	$\frac{L(\theta_{im}\gamma_{l,im}+(1-f)\rho_d\gamma_{s,im})}{\theta v c_0}$

The non-equilibrium models used were two-region (physical non-equilibrium) and two-site (chemical non-equilibrium). Using the dimensionless parameters listed in Table 3, both models reduce to the same dimensionless form (Equations (2) and (3)), where the subscripts 1 and 2 refer to either mobile and immobile regions for the two-region model (physical non-equilibrium) or the equilibrium and non-equilibrium sites for the two-site model (chemical non-equilibrium) [42]:

$$\beta R\frac{\partial C_1}{\partial T} = \frac{1}{Pe}\frac{\partial^2 C_1}{\partial Z^2} - \frac{\partial C_1}{\partial Z} - \omega(C_1 - C_2) - \mu_1 C_1 + \gamma_1(Z) \quad (2)$$

$$(1-\beta)R\frac{\partial C_2}{\partial T} = \omega(C_1 - C_2) - \mu_2 C_2 + \gamma_2(Z) \quad (3)$$

In Table 3, the subscripts "*im*" and "*m*" refer to the immobile and mobile regions, respectively. The two-region model is then referred to as the MIM model for Mobile-IMmobile water regions. The subscripts "*l*", "*s*", "*e*", and "*k*" refer to liquid phase, solid

phase, equilibrium, and kinetics, respectively. β is the dimensionless variable for partitioning in non-equilibrium transport models (either two-region or two-site); ω is the dimensionless mass transfer coefficient between the two regions or the two sites; C is the dimensionless resident concentration; μ is the first-order decay coefficient [T^{-1}]; γ is the zero-order production term [$ML^{-3}\ T^{-1}$]; v average pore-water velocity [$L\ T^{-1}$]; t is the time [T]; L is the characteristic length [L]; x is the distance [L]; D is the dispersion coefficient [$L^2\ T^{-1}$]; θ is the volumetric water content [$L^3\ L^{-3}$]; ρ_d is the bulk density [$M\ L^{-3}$]; f is the fraction of exchange sites assumed to be at equilibrium (two-site model) or the fraction of adsorption sites that equilibrates with the mobile liquid phase (two-region); K_d is the distribution coefficient for linear adsorption [$M^{-1}\ L^3$]; α is the first-order kinetic rate coefficient [T^{-1}]; R is the retardation faction; c is the volume-averaged or resident concentration of the liquid phase [$M\ L^{-3}$]; c_0 is the characteristic concentration for dimensionless parameters [$M\ L^{-3}$]; s is the concentration of the adsorbed phase [$M\ M^{-1}$].

2.4. Parameter Estimation

The transport parameters were determined using the STANMOD software, Versions 1.0 and 2.0 [43,44]. STANMOD software includes a modified and updated version of the CXTFIT code of Toride et al. [42] for estimating solute transport parameters using a nonlinear least-squares parameter optimization method. The transport parameters for KBr were obtained using the CDE model (with D and R as parameters) and the two-region MIM model (with D, R, β, and ω as related parameters). Bromide was considered a tracer without any reactivity. Conversely, RB5 was considered a reactive solute, and we used the two-site model to model RB5 BTCs.

2.5. Statistical Criteria

The following statistical criteria were used to analyze the quality of the fit of data to any of the models, i.e., the CDE, the two-region, and the two-site models: Mean Square Error (Equation (4)), Modeling Efficiency (Equation (5)), Deviation Ratio (Equation (6)), and Residual Mass Coefficient (Equation (7)).

$$MSE = \left(\frac{\sum_{i=1}^{N} (T_i - M_i)^2}{N} \right)^{\frac{1}{2}} \cdot \frac{100}{M} \tag{4}$$

$$ME = \frac{\sum_{i=1}^{N} (M_i - \overline{M})2 - \sum_{i=1}^{N} (T_i - M_i)^2}{\sum_{i=1}^{N} (M_i - M)^2} \tag{5}$$

$$DR = \frac{\sum_{i=1}^{N} (M_i - \overline{M})2}{\sum_{i=1}^{N} (T_i - \overline{M})2} \tag{6}$$

$$RMC = \frac{\sum_{i=1}^{N} M_i - \sum_{i=1}^{N} T_i}{\sum_{i=1}^{N} M_i} \tag{7}$$

where T_i is the values calculated by the model, M_i is the experimental values, $\overline{M}$ is the average of the observed values, and n is the number of data points.

The criterion DR describes the ratio of the experimental values' dispersion to theoretical values (i.e., modeled values). DR should be close to unity for good fits. In the absence of systematic deviations between the theoretical and experimental values, the criterion RMC should tend to zero. RMC indicates whether the model tends to overestimate or underestimate the observations according to its signs: negative values for overestimation and positive values for underestimation. The MSE indicates the degree of deviation between the experimental and the modeled values. This criterion should tend to zero for good fit. The ME criterion indicates whether the theoretical model provides a better estimation of the experimental values than the mean value of these observations. Its values should be close to one [18].

The determination coefficient (R^2) was also used to assess the quality of the statistical adjustments (Equation (8)). R^2 determines the variance in the experienced observations that can be explained by the model, thereby expecting a value of 1 for good values.

$$R^2 = 1 - \frac{SQ_E}{SQ_T} \quad (8)$$

where SQ_E is the sum of the residue squares, and SQ_T is the sum of the total square values.

3. Results and Discussion

3.1. KBR Transport

The values of the variables determined experimentally for the KBr transport tests performed at the concentration of 0.3 mol L^{-1} and the flow rate of 0.32 mL min^{-1} are shown in Table 4. The standard deviations were minor compared to the order of magnitude, indicating that the repetitions were of good quality and representative of the averaged behavior.

Table 4. Experimental conditions for the miscible displacement tests for CM1 and CM2.

Layer	ρ_d (g cm^{-3})	V_p (cm^3)	θ (cm^3 cm^{-3})	q (cm h^{-1})	v (cm h^{-1})	T_{pulse} (h)
CM1	1.515 ± 0.002	36.453 ± 0.242	0.343 ± 0.002	3.723 ± 0.004	10.846 ± 0.077	1.930 ± 0.047
CM2	1.627 ± 0.002	37.533 ± 0.153	0.357 ± 0.003	3.625 ± 0.118	10.153 ± 0.304	1.975 ± 0.019

Average ± standard deviation, ρ_d: density; V_p: pore volume; θ: porosity; q: Darcy flux; v: average pore water velocity; T_{pulse}: displacement time of 1 pore volume.

The BTCs observed and fitted by CXTFIT are shown in Figure 3. Fitted transport parameters are presented in Tables 5 and 6, together with the determination coefficients, R^2, and the statistical parameters, respectively, for the CDE and the two-region models.

Table 5. Estimated values of parameters, determination coefficient R^2, and statistical criteria for the CDE model for KBr transfer in the soils CM1 and CM2 for the tracer (KBr).

Layer	D (cm^2 h^{-1})	R	λ (cm)	Pe	R^2	MSE	DR	ME	RMC
CM1	3.512 ± 0.427	1.010 ± 0.019	0.324 ± 0.040	62.353 ± 7.410	0.983 ± 0.004	14.927 ± 2.597	0.921 ± 0.001	0.984 ± 0.004	0.005 ± 0.007
CM2	5.559 ± 0.692	0.741 ± 0.021	0.547 ± 052	36.796 ± 3.324	0.967 ± 0.001	19.037 ± 0.910	0.894 ± 0.044	0.968 ± 0.001	0.038 ± 0.025

Average ± standard deviation.

Table 6. Estimated parameters, determination coefficient R^2, and statistical criteria for the two-region model for CM1 and CM2 for the tracer (KBr).

Layer	D (cm^2 h^{-1})	R	λ (cm)	β	ω	Pe	R^2	MSE	DR	ME	RMC
CM1	1.023 ± 0.359	1.065 ± 0.023	0.101 ± 0.036	0.880 ± 0.018	0.018 ± 0.004	228.586 ± 71.797	0.997 ± 0.002	6.235 ± 3.012	1.010 ± 0.003	0.997 ± 0.002	0.003 ± 0.007
CM2	5.151 ± 0.504	0.790 ± 0.017	0.507 ± 0.047	0.806 ± 0.010	0.019 ± 0.002	39.638 ± 3.527	0.991 ± 0.001	9.640 ± 0.199	1.023 ± 0.010	0.992 ± 0.001	0.047 ± 0.013

Average ± standard deviation.

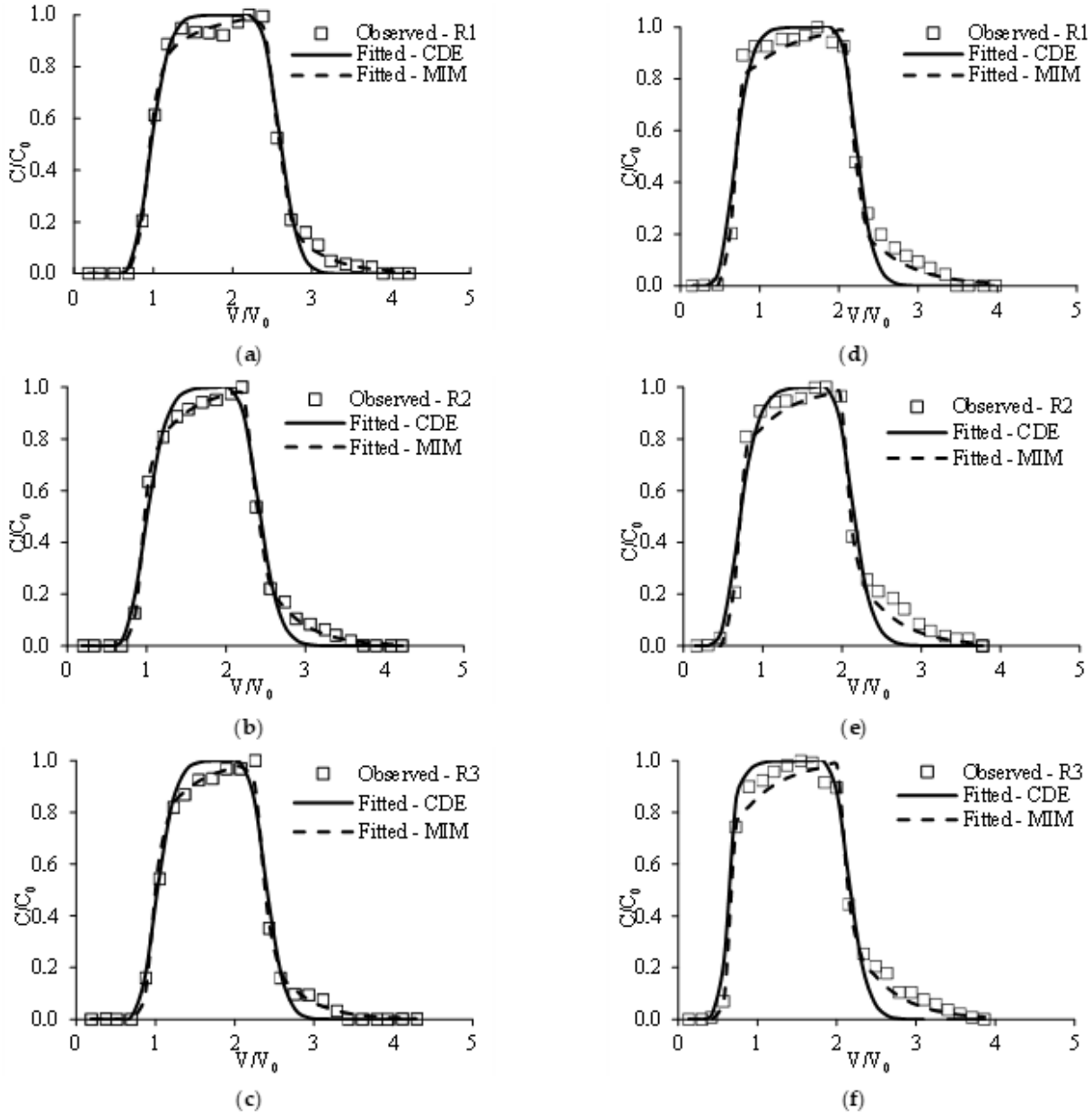

Figure 3. KBr observed and fitted breakthrough curves (BTCs) for the CDE and MIM models two-region models CM1 (**a**–**c**) and CM2 (**d**–**f**).

The BTCs for soil CM1 (Figure 3) pass through point $V/V_0 = 1.0$ and $C/C_0 = 0.5$, which is the theoretical condition for an ideal tracer. However, this fact did not occur for soil CM2, for which the BTCs were slightly shifted to the left of point $V/V_0 = 1.0$ and $C/C_0 = 0.5$. In addition, the BTCs were asymmetric and exhibited significant tailing for both soils. Similar behaviors were observed by Costa et al. [45] for the transport of KBr in alluvial soil. These authors concluded that water fractionation into mobile–immobile regions (physical non-equilibrium) requires the use of the two-region model. Dousset et al. [46] also observed that the equilibrium transport CDE model did not reproduce BTC tailing for their studied soil (a silty clay loam). The modeling clearly shows that the two-region model better fits the BTC peak for the two studied soils. Additionally, the adequacy of the two-region model, as shown in Figure 3, is consistent with the values of R^2 with higher values for the two-region model in comparison to the CDE model (Table 6 versus Table 5). The values were higher than 0.99 for the two-region model and provided valid estimations of the related transport

parameters. The other statistical parameters (MSE, DR, ME, and RMC) confirmed the two-region model's gain in describing the experimental BTCs.

The analysis of BTCs gives further insight into bromide transfer. When the BTC passes by point $V/V_0 = 1.0$ and $C/C_0 = 0.5$, the retardation faction (R) is equal to 1. When they are shifted to the left, retardation factors are below unity, which was confirmed by their values (Table 6). Values of R lower than unity were also found for KBr in a vertisol by Milfont et al. [33] and in loamy sand soil by Carmo et al. [36]. This feature indicates that bromide elutes through the column faster than water, often attributed to anionic exclusion or isolated volumes of water in the columns [28,47,48]. Prédélus et al. [49], who investigated the effect of the soil structure and texture on the transport of bromide and colloidal particles under unsaturated conditions and concluded that the fine soil particles promoted anionic exclusion. Therefore, considering the low percentage of fine particles in our soils and the physical non-equilibrium already identified, we favor the hypothesis of anionic exclusion resulting from the flow field and the presence of isolated pockets of water.

The estimations of the dispersion coefficient, D, show higher values for soil CM2 (5.151 $cm^2\ h^{-1}$) in comparison to soil CM1 (1.023 $cm^2\ h^{-1}$) (Table 6). This fact may result from the soil granulometry, with a coarser texture for soil CM2 with 95.480% of sand, 4.205% of silt, and 0.315% of clay, versus 79.395% of sand, 15.710% of silt, and 4.895% of clay. The λ values score 0.101 cm for CM1 and 0.507 cm for CM2 (Table 6), confirming more solute dispersion in soil CM2. These values are in the same order of magnitude as those found by Sidoli et al. [28], who found a value of 0.50 cm for bromide transport in sandy soil (95.7% of sand) under unsaturated conditions. The values of λ are also indicative of the particle size distribution and homogeneity [50,51].

The Peclet number, P_e, gives insight into the relative importance of advective and dispersive processes [52]. In the diffusion-dominated regime, $P_e \leq 0.1$, advection is negligible. Conversely, $P_e > 300$ corresponds to the mechanical dispersion regime with the predominance of advection. The intermediate values, $10 < P_e < 100$, indicate the power-law dispersion regime [53,54]. P_e values found in our study for KBr move away from the intermediary conditions for CM1, with $P_e = 228.586$ (Table 6), tending toward purely advective transport. For CM2, $P_e = 39.638$ (Table 6), which corresponds to the intermediate power law dispersion regime.

The dimensionless partitioning coefficient β indicates the proportion of mobile water, while the mass transfer coefficient ω describes the exchange rate between the immobile and mobile regions. The estimated values of β are 0.880 for soil CM1 and 0.806 for soil CM2 (Table 6). These values imply that about 12% and 20% of the water is immobile in the columns for CM1 and CM2. This means that in CM1, flow is more homogeneous, and the pores are more accessible to solutes. Conversely, in soil CM2, a greater volume of pores remains accessible to solute by solute diffusion. However, these immobile water fractions remain relatively low in comparison to coarse soils prone to preferential flows [48] or soil with macropores [55]. Lastly, the parameter ω takes similar values for the two soils, with 0.018 for CM1 and 0.019 for CM2. These small values suggest that solute diffusion is slow at the interface between mobile and immobile regions, with local physical non-equilibrium [56].

3.2. Miscible Displacement of Dye RB5 in Alluvial Soil

The RB5 observed and fitted by the two-site model are shown in Figure 4. In Table 7, the transport parameters provided by the two-site model are presented. In comparison to KBr transport, RB5 exhibited different BTCs (Figure 4 versus Figure 3). The RB5 BTCs were asymmetric and showed significant tailing for both soils, indicating chemical non-equilibrium in addition to physical equilibrium. For the sake of simplicity, we neglected physical non-equilibrium and considered only chemical non-equilibrium. Thus, the two-site model (chemical non-equilibrium) was used to model the RB5 BTCs, and accurate fits were obtained with the parameters tabulated in Table 6. A slight discrepancy between the observed and adjusted peaks was observed in some repetitions of CM1 and CM2. However,

these discrepancies were small in all cases, and the suitability of the two-site model was confirmed by the values of R2 (Table 7). The MSE and RMC statistics, which have an expected value of 0, and DR and ME, which have an expected value of 1, also validate the accuracy of the two-site model.

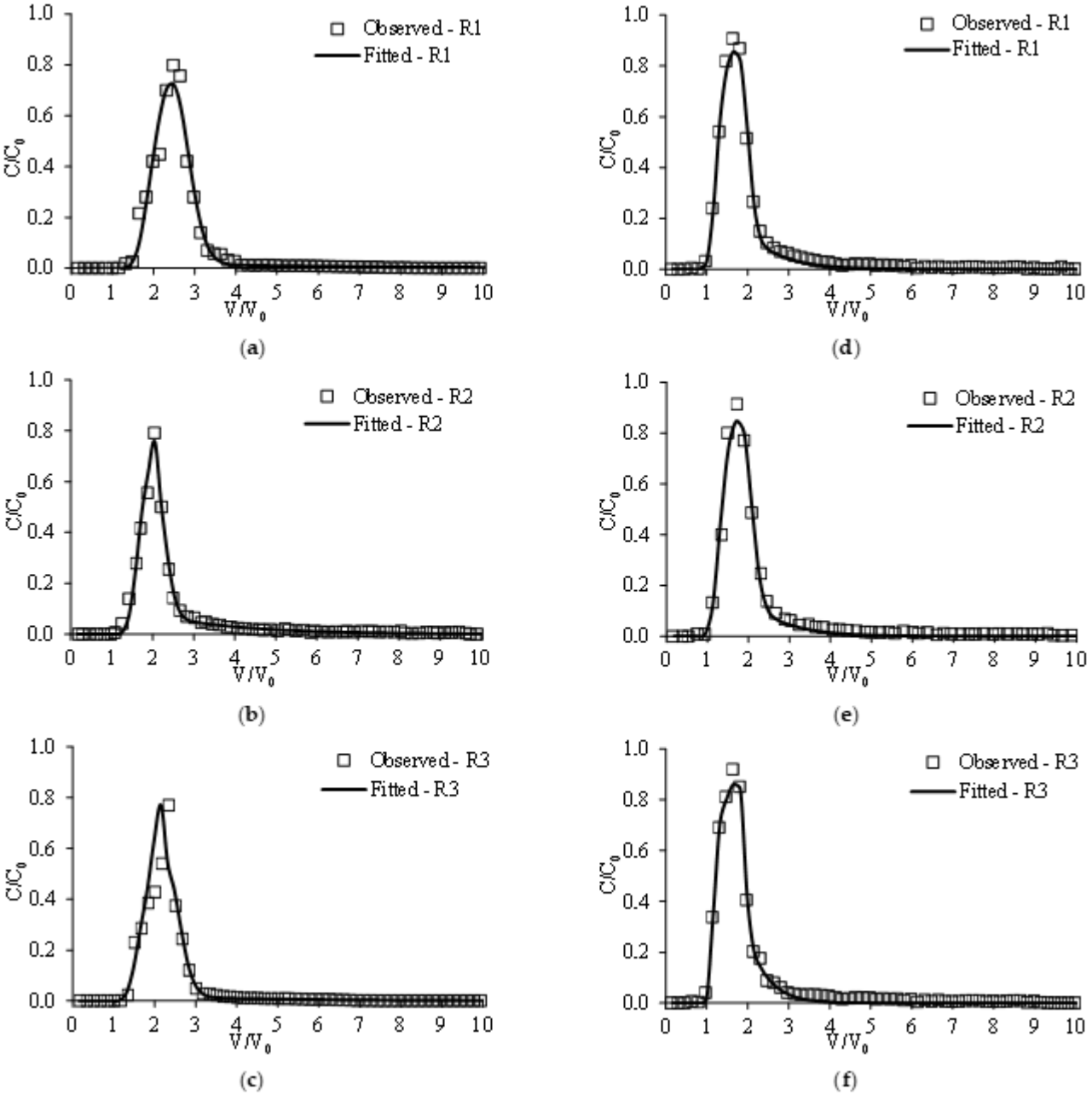

Figure 4. RB5 BTCs observed and fitted by CXTFIT for two-site model CM1 (**a**–**c**) and CM2 (**d**–**f**).

The asymmetry of the curves was attributed to the reactivity between the dye and the soils, so that about six pore volumes were needed to elute the dye fully in columns CM1 and CM2. The relative peak concentration (C/C_0) for CM1 was between 0.7 and 0.8, and for CM2, it was approximately 0.9. Furthermore, the peaks of the curves were shifted to the right of point $V/V_0 = 1.0$ and $C/C_0 = 0.5$ when compared to the KBr BTCs. The reactivity of the dye RB5 with the soils caused a delay in its elution at the column outlet. In accordance, the R values were greater than 1, i.e., 8.993 for CM1 and 3.333 for CM2 (Table 7). In addition, the R values were higher for CM1 than for CM2, revealing more interaction between the

RB5 dye and the superficial layer. Indeed, the mobility of solutes is inversely related to their adsorption. In batch tests conducted with the same soils for the dye RB5 [12] and the Direct Black 22 dye [17], more significant adsorption of the mentioned dyes was also observed for soil CM1. Thus, it was expected that the retention of dye RB5 was higher in CM1, and its mobility was more elevated in CM2.

Table 7. Estimated values of parameters, determination coefficient R^2 and MSE, DR, ME, and RMC statistical criteria for the two-site model for CM1 and CM2.

Layer	D ($cm^2\ h^{-1}$)	*R*	β	ω	R^2	MSE	DR	ME	RMC
CM1	2.253 ± 0.406	8.993 ± 0.327	0.216 ± 0.080	0.015 ± 0.006	0.979 ± 0.002	38.968 ± 2.077	1.028 ± 0.116	0.972 ± 0.077	−0.004 ± 0.004
CM2	2.796 ± 0.322	3.333 ± 0.094	0.351 ± 0.010	0.015 ± 0.007	0.966 ± 0.002	59.623 ± 2.695	1.047 ± 0.106	0.949 ± 0.018	−0.071 ± 0.031

Average ± standard deviation.

The processes involved in the transport of RB5 in soil columns can be linked to the characteristics of the soil (Table 1). The greater or lesser retention of RB5 in soils is related to soil properties, such as pH, ZPC (Zero Point Charge), organic and clay contents, and CEC. The pH of CM1 is higher than the ZPC value, and for CM2, the value is approximately equal, indicating that the analyzed soils have a low retention potential for anionic RB5. For a pH lower than ZPC, the matrix particles are expected to be positively charged. Conversely, for pHs higher than ZPC, the particle surfaces are expected to be negatively charged [23]. The first condition attracts anions, and the second one attracts cations [5]. For example, Dawodu and Akpomie [57], who analyzed the sorption of the anionic dye Acid Yellow 23 in soils, observed that optimal sorption occurred at a pH lower than the soil ZPC.

Studies have also shown the influence of soil organic content on anionic dye sorption [12,58]. For example, regarding this component, Liu et al. [58] verified a decrease in sorption of the anionic dyes Mordant Black 11 and Direct Blue 86 (25% and 40%, respectively) in a fluvial soil after OC removal by H_2O_2 treatment. Besides the organic content, dye molecules, in general, have a strong affinity with clay minerals [12]. While clay has a higher capacity for cation exchange than for anion exchange due to its negatively charged particles [59], studies positively correlate the RB5 dye sorption with the clay content of soils [12,60]. At that point, the presence of kaolinite with acid surfaces favors the sorption of anionic dyes because these minerals constitute the main adsorbent sites for these dyes [59]. The analyzed soils present low OC (1.26% and 0.97%, for CM1 and CM2, respectively) and low clay content (4.895% and 0.315%, respectively), which explains the low retention and high mobility verified. The high CEC values indicate that attract and fix positively charged elements [61] with opposite trends for anions. Thus, it is possible to infer from the CEC that the analyzed soils do not present favorable conditions for considerable retention of the anionic RB5, which also justifies the high mobility and low retention verified.

Both β (0.216 for the CM1 and 0.351 for the CM2) and ω (0.015 for the CM1 and 0.015 for the CM2) were lower than 1, indicating a rate-limited adsorption process [31]. In the two-site sorption model, parameter β is a partition coefficient, which indirectly represents the fraction of the sites available for instantaneous sorption [32]. The β values derived from BTC indicate that about 21% and 35% corresponded to instantaneous adsorption, respectively, for CM1 and CM2, the rest being impacted by kinetics. The ω values were significantly small, indicating slow retention processes.

The existence of physical non-equilibrium observed in the experiments with KBr demonstrates the possibility of the presence of a non-uniformity in the water flow generated by the existence of macropores and high structural heterogeneity of the lithofacies, which are predominantly sandy in the alluvial deposits. Such behavior has frequently been observed in sandy soils in sedimentary environments [18,35,62–64]. The non-uniformity in the water flow can directly impact the RB5 transport processes in the natural environment,

generating greater complexity in the RB5 sorption processes, mainly due to the contrast between the transport parameters obtained for the applied models.

In general, the parameters obtained demonstrate a low retention capacity of RB5 and a high displacement capacity for the deeper layers. This indicates a high risk of aquifer contamination, making the management of water use in these formations difficult for the diffuse population in the Brazilian semi-arid region. In addition, the present work has a peculiar focus on RB5 dye. However, textile effluents are presented in the form of a mixture of several dyes, which can have a much greater impact on groundwater quality. Despite the institutional mechanisms present in Brazilian legislation, inspection actions for the release of industrial effluents are still a great challenge, requiring practical public policies to maintain water quality, especially in semi-arid regions, such as northeast Brazil.

Future investigations can be carried out to evaluate RB5 transport processes at the field scale, for example, the use of two-dimensional or three-dimensional numerical simulation tools. The parameters obtained on the small scale (Batch) and on the macro scale (column tests) can be coupled to these numerical models, aiming to simultaneously simulate the transfer of water and the transport of RB5 based on a more detailed description of the sedimentary deposit of the point from a structural point of view. The use of more detailed information on the architecture of the alluvial deposit is fundamental for the success of this type of investigation, especially the more accurate knowledge of the degree of heterogeneity of the deposit, resulting in a more realistic assessment of the behavior of RB5 on a large scale.

The existing discontinuity between the hydrodynamic and transport properties of the alluvial deposit layers added to the observed physical and chemical non-equilibrium phenomena suggests that the large-scale RB5 transport processes may be influenced by preferential flows. In addition, the dynamics of the RB5 transport processes in the alluvium may have different behaviors depending on climatic seasonality. In this context, future research will be able to assess the context of the propagation dynamics of the RB5 contamination plume in two scenarios: (i) In long periods of drought in the semi-arid region, with occasional rainfall and pollutant transport mechanisms in an unsaturated medium. (ii) Soon after the occurrence of floods, where the flow on the surface can be more severe due to hydraulic head and related activation of macropores and fractures, as a transport mechanism of pollutants in a highly heterogeneous medium and under saturation conditions.

4. Conclusions

Miscible displacement tests were conducted under saturated conditions to understand the environmental performance and risks associated with contamination by RB5 dye in the alluvial soils of Alto Capibaribe (Brazil). The percolation test was also carried out for the non-reactive tracer KBr to characterize the flow pattern.

Physical non-equilibrium was found in the soils for KBr transport, and the two-region model adequately modeled the experimental breakthrough curves (BTCs). For the transport of RB5, the results showed a chemical non-equilibrium, much stronger than the physical non-equilibrium, and the two-site model was considered and adequately modeled the experimental BTCs.

The results indicate that the surface soil layer is the most reactive, with stronger retention of RB5. However, both layers showed low retention and high mobility for RB5. These results are worrying because they point to the rapid and efficient transfer to deeper soil horizons and potentially groundwater. The studied alluvial deposit presents coarse-grained materials in its composition, low organic matter content, and insignificant clay content, and thus is prone to downward transfer on anions, increasing the risk of groundwater contamination. In addition, the difference in the retention capacity of the soil layers points to the need to investigate solute and pollutant transfer in heterogeneous porous media.

This study is promising for studying fluxes in other sedimentary environments, notably alluvial deposits from the semi-arid northeast. It is essential to better understand the fluxes in the alluvial deposit to correctly describe and predict the fate of the pollutant that infiltrates deeper underground layers. Thus, it is suggested that future work analyze the deeper layers of the alluvium to complete the understanding of the dissipation of RB5. It is also recommended that studies similar to this study be conducted for other textile dyes used by the local textile industry coexisting in the same solution and at different concentrations to simulate different characteristics of the real textile effluent.

Author Contributions: Conceptualization, A.T.A.A., A.P.C. and S.M.d.S.N.; methodology, A.T.A.A., V.H.d.O.B. and S.M.d.S.N.; software, A.T.A.A. and A.P.C.; validation, A.T.A.A., V.H.d.O.B. and A.P.C.; formal analysis, A.T.A.A.; investigation, A.T.A.A. and S.M.d.S.N.; resources, A.P.C. and J.R.d.S.L.; data curation, A.T.A.A. and V.H.d.O.B.; writing—original draft preparation, A.T.A.A. and L.L.; writing—review and editing, A.P.C., A.C.D.A., J.R.d.S.L. and L.L.; visualization, A.T.A.A.; supervision, A.P.C., L.L. and A.C.D.A.; project administration, A.P.C., A.C.D.A. and J.R.d.S.L.; funding acquisition, A.P.C. and A.C.D.A. All authors have read and agreed to the published version of the manuscript.

Funding: This study was financed in part by the Coordenação de Aperfeiçoamento de Pessoal de Nível Superior-Brasil (CAPES)-Finance Code 001 and of the Pró-Reitoria de Pós-Graduação of the Federal University of Pernambuco (PROPG-UFPE).

Acknowledgments: This work was carried out with the support of the following projects: "Transfer of Water and Mixtures of Reactive Pollutants in Anthropized Soils" (CNPq process No. 436875/2018-7); "National Observatory of Water and Carbon Dynamics in the Caatinga Biome ONDACBC (CNPq process No. 465764/2014-2; CAPES process No. 88887.136369/2017-00; FACEPE process APQ-0498-3.07/17); "Water and Carbon Dynamics in the Caatinga Biome" (UFPE/PRINT-CAPES Process No. 88881.318207/2019-01). The authors are also grateful for the master grant of the first author (FACEPE process IBPG-0125-3.01/17) and to CNPq for the PQ grant (Research and Productivity) of the second author (CNPq Process No. 315927/2021-6).

Conflicts of Interest: The authors declare no conflict of interest.

References

1. Huynh, N.-T.; Chien, C.-F. A Hybrid Multi-Subpopulation Genetic Algorithm for Textile Batch Dyeing Scheduling and an Empirical Study. *Comput. Ind. Eng.* **2018**, *125*, 615–627. [CrossRef]
2. Nazmul Islam, G.M.; Ke, G.; Ahsanul Haque, A.N.M.; Azharul Islam, M. Effect of Ultrasound on Dyeing of Wool Fabric with Acid Dye. *Int. J. Ind. Chem.* **2017**, *8*, 425–431. [CrossRef]
3. Liu, Y.; Shao, Z.; Reng, X.; Zhou, J.; Qin, W. Dye-Decolorization of a Newly Isolated Strain Bacillus Amyloliquefaciens W36. *World J. Microbiol. Biotechnol.* **2021**, *37*, 8. [CrossRef]
4. Hanafi, M.F.; Sapawe, N. Effect of pH on the Photocatalytic Degradation of Remazol Brilliant Blue Dye Using Zirconia Catalyst. *Mater. Sci. Proc.* **2020**, *31*, 260–262. [CrossRef]
5. Banerjee, S.; Chattopadhyaya, M.C. Adsorption Characteristics for the Removal of a Toxic Dye, Tartrazine from Aqueous Solutions by a Low Cost Agricultural by-Product. *Arab. J. Chem.* **2017**, *10*, S1629–S1638. [CrossRef]
6. Stagnaro, S.M.; Volzone, C.; Huck, L. Nanoclay as Adsorbent: Evaluation for Removing Dyes Used in the Textile Industry. *Procedia Mater. Sci.* **2015**, *8*, 586–591. [CrossRef]
7. Jayanthy, V.; Geetha, R.; Rajendran, R.; Prabhavathi, P.; Sundaram, S.K.; Kumar, S.D.; Santhanam, P. Phytoremediation of Dye Contaminated Soil by *Leucaena leucocephala* (Subabul) Seed and Growth Assessment of *Vigna radiata* in the Remediated Soil. *Saudi J. Biol. Sci.* **2014**, *21*, 324–333. [CrossRef] [PubMed]
8. Kharat, D. Treatment of Textile Industry Effluents: Limitations and Scope. *J. Environ. Res. Dev.* **2015**, *9*, 1210.
9. Smaranda, C.; Popescu, M.-C.; Bulgariu, D.; Măluţan, T.; Gavrilescu, M. Adsorption of Organic Pollutants onto a Romanian Soil: Column Dynamics and Transport. *Process. Saf. Environ. Prot.* **2017**, *108*, 108–120. [CrossRef]
10. Rehman, K.; Shahzad, T.; Sahar, A.; Hussain, S.; Mahmood, F.; Siddique, M.H.; Siddique, M.A.; Rashid, M.I. Effect of Reactive Black 5 Azo Dye on Soil Processes Related to C and N Cycling. *PeerJ* **2018**, *6*, e4802. [CrossRef]
11. Louati, I.; Elloumi-Mseddi, J.; Cheikhrouhou, W.; Hadrich, B.; Nasri, M.; Aifa, S.; Woodward, S.; Mechichi, T. Simultaneous Cleanup of Reactive Black 5 and Cadmium by a Desert Soil Bacterium. *Ecotoxicol. Environ. Saf.* **2020**, *190*, 110103. [CrossRef] [PubMed]
12. Alves, A.T.A.; de Souza Silva, L.T.M.; de Alcântara, L.R.P.; de Oliveira Barros, V.H.; dos Santos, S.M.; de Lima, V.F.; de Sousa Lima, J.R.; Coutinho, A.P.; Antonino, A.C.D. Sorption of Remazol Black B Dye in Alluvial Soils of the Capibaribe River Basin, Pernambuco, Brazil. *Rev. Ambiente Água* **2020**, *15*. [CrossRef]

13. Lai, K.C.; Lee, L.Y.; Hiew, B.Y.Z.; Yang, T.C.-K.; Pan, G.-T.; Thangalazhy-Gopakumar, S.; Gan, S. Utilisation of Eco-Friendly and Low Cost 3D Graphene-Based Composite for Treatment of Aqueous Reactive Black 5 Dye: Characterisation, Adsorption Mechanism and Recyclability Studies. *J. Taiwan Inst. Chem. Eng.* **2020**, *114*, 57–66. [CrossRef]
14. Felista, M.M.; Wanyonyi, W.C.; Ongera, G. Adsorption of Anionic Dye (Reactive Black 5) Using Macadamia Seed Husks: Kinetics and Equilibrium Studies. *Sci. Afr.* **2020**, *7*, e00283. [CrossRef]
15. El Bouraie, M.; El Din, W.S. Biodegradation of Reactive Black 5 by Aeromonas Hydrophila Strain Isolated from Dye-Contaminated Textile Wastewater. *Sustain. Environ. Res.* **2016**, *26*, 209–216. [CrossRef]
16. Braga, R.A.P.; de Oliveira Farias, C.; da Silva, S.; Cavalcanti, E.R. *Gestão e Educação Socioambiental Na Bacia Do Capibaribe*; Clã, Ed.; ANE Publishing: Recife, Brazil, 2015; p. 140.
17. Da Silva Alexandre, J.I.; dos Santos, S.M.; Coutinho, A.P.; de Melo, T.d.A.T.; Gonçalves, E.A.P.; Gondim, M.V.S.; Antonino, A.C.D.; da Cunha Rabelo, A.E.C.d.G.; de Oliveira, A.L. Sorption of the Direct Black 22 Dye in Alluvial Soil. *Rev. Ambiente Água* **2020**, *15*. [CrossRef]
18. Da Cunha Rabelo, A.E.C.d.G.; dos Santos Neto, S.M.; Coutinho, A.P.; Antonino, A.C.D. Sorption of Sulfadiazine and Flow Modeling in an Alluvial Deposit of a Dry Riverbed in the Brazilian Semiarid. *J. Contam. Hydrol.* **2021**, *241*, 103818. [CrossRef]
19. Febrianto, G.; Karisma, D.; Mangindaan, D. Polyetherimide Nanofiltration Membranes Modified by Interfacial Polymerization for Treatment of Textile Dyes Wastewater. *IOP Conf. Ser. Mater. Sci. Eng.* **2019**, *622*, 012019. [CrossRef]
20. Zhu, J.; Qin, L.; Uliana, A.; Hou, J.; Wang, J.; Zhang, Y.; Li, X.; Yuan, S.; Li, J.; Tian, M.; et al. Elevated Performance of Thin Film Nanocomposite Membranes Enabled by Modified Hydrophilic MOFs for Nanofiltration. *ACS Appl. Mater. Interfaces* **2017**, *9*, 1975–1986. [CrossRef]
21. Sana, D.; Jalila, S. Combined Effect of Unsaturated Soil Condition and Soil Heterogeneity on Methylene Blue Adsorption/Desorption and Transport in Fixed Bed Column: Experimental and Modeling Analysis. *J. King Saud Univ. Sci.* **2016**, *28*, 308–317. [CrossRef]
22. Smaranda, C.; Gavrilescu, M.; Bulgariu, D. Studies on Sorption of Congo Red from Aqueous Solution onto Soil. *Int. J. Environ. Res.* **2011**, *5*, 177–188. [CrossRef]
23. Bachratá, M.; Šuňovská, A.; Horník, M.; Pipíška, M.; Augustín, J. Sorption of Synthetic Dyes Onto River Sediments: A Laboratory Study. *Nova Biotechnol. Chim.* **2013**, *12*, 12–29. [CrossRef]
24. Zhang, X.; Tong, J.; Hu, B.X.; Wei, W. Adsorption and Desorption for Dynamics Transport of Hexavalent Chromium (Cr(VI)) in Soil Column. *Environ. Sci. Pollut. Res.* **2018**, *25*, 459–468. [CrossRef] [PubMed]
25. Dong, Z.; Wei, L.; Xu, S.; Sun, J.; Shi, X.; Qiu, Y. Transport of Imidazolium-Based Ionic Liquids with Different Anion/Cation Species in Sand/Soil Columns. *Ecotoxicol. Environ. Saf.* **2018**, *147*, 480–486. [CrossRef] [PubMed]
26. Palácio Filho, A.M.; Netto, A.M.; Corrêa, M.M.; Neto, F.C.R.; Da Silva, L.P.; Malta, S.H.D.S. Hydrodynamic and Hydrodispersive Characterization of a Fluvic Cambisol in the Northeast Region of Brazil. *Rev. Caatinga* **2020**, *33*, 160–171. [CrossRef]
27. Šimůnek, J.; van Genuchten, M.T. Modeling Nonequilibrium Flow and Transport Processes Using HYDRUS. *Vadose Zone J.* **2008**, *7*, 782–797. [CrossRef]
28. Sidoli, P.; Lassabatere, L.; Angulo-Jaramillo, R.; Baran, N. Experimental and Modeling of the Unsaturated Transports of S-Metolachlor and Its Metabolites in Glaciofluvial Vadose Zone Solids. *J. Contam. Hydrol.* **2016**, *190*, 1–14. [CrossRef] [PubMed]
29. Van Genuchten, M.T.; Wierenga, P.J. Mass Transfer Studies in Sorbing Porous Media I. Analytical Solutions. *Soil Sci. Soc. Am. J.* **1976**, *40*, 473–480. [CrossRef]
30. Gao, G.; Zhan, H.; Feng, S.; Fu, B.; Ma, Y.; Huang, G. A New Mobile-Immobile Model for Reactive Solute Transport with Scale-Dependent Dispersion. *Water Resour. Res.* **2010**, *46*. [CrossRef]
31. Cao, Y.; Dong, S.; Dai, Z.; Zhu, L.; Xiao, T.; Zhang, X.; Yin, S.; Soltanian, M.R. Adsorption Model Identification for Chromium (VI) Transport in Unconsolidated Sediments. *J. Hydrol.* **2021**, *598*, 126228. [CrossRef]
32. Florido, A.; Valderrama, C.; Arévalo, J.A.; Casas, I.; Martínez, M.; Miralles, N. Application of Two Sites Non-Equilibrium Sorption Model for the Removal of Cu(II) onto Grape Stalk Wastes in a Fixed-Bed Column. *Chem. Eng. J.* **2010**, *156*, 298–304. [CrossRef]
33. Milfont, M.L.; Antonino, A.C.; Martins, J.M.; Netto, A.M.; Corrêa, M.M. Caracterização Hidrodispersiva de Dois Solos Do Vale Do Rio São Francisco. *Rev. Bras. Ciênc. Agrár.* **2006**, *1*, 81–87. [CrossRef]
34. Milfont, M.L.; Antonino, A.C.D.; Martins, J.M.F.; Netto, A.M.; Gouveia, E.R.; Correa, M.M. Transporte Do Paclobutrazol Em Colunas de Solos. *Rev. Bras. Ciênc. Solo* **2008**, *32*, 2165–2175. [CrossRef]
35. Winiarski, T.; Lassabatere, L.; Angulo-Jaramillo, R.; Goutaland, D. Characterization of the Heterogeneous Flow and Pollutant Transfer in the Unsaturated Zone in the Fluvio-Glacial Deposit. *Procedia Environ. Sci.* **2013**, *19*, 955–964. [CrossRef]
36. Do Carmo, A.I.; Antonino, A.C.D.; Martins, J.M.F.; da Silva, V.L.; Morel, M.C.; Gaudet, J.P. Lixiviação de Naftaleno Em Solos Urbanos Da Região Metropolitana Do Recife, PE. *Rev. Bras. Ciênc. Solo* **2013**, *37*, 1415–1422. [CrossRef]
37. Moura, A.; Carvalho, J.; Montenegro, S.; Carmo, A.; Magalhães, A.; Sousa, C.; Antonino, A.; Araujo, J.; Melo, R. Determinação de Parâmetros Hidrodispersivos Em Solos Da Zona Da Mata de Pernambuco. *Rev. Bras. Recur. Hídricos* **2013**, *18*, 109–115. [CrossRef]
38. Do Carmo, A.I.; Antonino, A.C.; Netto, A.M.; Corrêa, M.M. Caracterização Hidrodispersiva de Dois Solos Da Região Irrigada Do Vale Do São Francisco. *Rev. Bras. Eng. Agríc. Ambient.* **2010**, *14*, 698–704. [CrossRef]
39. Prédélus, D.; Coutinho, A.P.; Lassabatere, L.; Bien, L.B.; Winiarski, T.; Angulo-Jaramillo, R. Combined Effect of Capillary Barrier and Layered Slope on Water, Solute and Nanoparticle Transfer in an Unsaturated Soil at Lysimeter Scale. *J. Contam. Hydrol.* **2015**, *181*, 69–81. [CrossRef]

40. Ben Dassi, R.; Chamam, B.; Méricq, J.P.; Faur, C.; El Mir, L.; Trabelsi, I.; Heran, M. Novel Polyvinylidene Fluoride/Lead-Doped Zinc Oxide Adsorptive Membranes for Enhancement of the Removal of Reactive Textile Dye. *Int. J. Environ. Sci. Technol.* **2021**, *18*, 2793–2804. [CrossRef]
41. Vanderborght, J.; Vereecken, H. Review of Dispersivities for Transport Modeling in Soils. *Vadose Zone J.* **2007**, *6*, 29–52. [CrossRef]
42. Toride, N.; Leij, F.; Van Genuchten, M.T. *The CXTFIT Code for Estimating Transport Parameters from Laboratory or Filed Tracer Experiments*; US Salinity Laboratory: Riverside, CA, USA, 1995.
43. Simunek, J.; Van Genuchten, M.T.; Sejna, M.; Toride, N.; Leij, F. *The STANMOD Computer Software for Evaluating Solute Transport in Porous Media Using Analytical Solutions of Convection-Dispersion Equation. Versions 1.0 and 2.0*; Rep. IGWMC-TPS; IGWMC: Golden, CO, USA, 1999; p. 32.
44. Van Genuchten, M.T.; Šimunek, J.; Leij, F.J.; Toride, N.; Šejna, M. STANMOD: Model Use, Calibration, and Validation. *Trans. ASABE* **2012**, *55*, 1355. [CrossRef]
45. Costa, C.T.; Antonino, A.C.D.; Netto, A.M. Ensaios de Deslocamento de Líquido Miscível Na Determinação Dos Parâmetros Hidrodispersivos de Um Solo Aluvial. *Rev. Bras. Recur. Hídricos* **2006**, *11*, 111–122.
46. Dousset, S.; Thevenot, M.; Pot, V.; Simunek, J.; Andreux, F. Evaluating Equilibrium and Non-Equilibrium Transport of Bromide and Isoproturon in Disturbed and Undisturbed Soil Columns. *J. Contam. Hydrol.* **2007**, *94*, 261–276. [CrossRef] [PubMed]
47. Lassabatere, L.; Spadini, L.; Delolme, C.; Février, L.; Galvez-Cloutier, R.; Winiarski, T. Concomitant Zn-Cd and Pb Retention in a Carbonated Fluvio-Glacial Deposit under Both Static and Dynamic Conditions. *Chemosphere* **2007**, *69*, 1499–1508. [CrossRef] [PubMed]
48. Lassabatere, L.; Winiarski, T.; Galvez Cloutier, R. Retention of Three Heavy Metals (Zn, Pb, and Cd) in a Calcareous Soil Controlled by the Modification of Flow with Geotextiles. *Environ. Sci. Technol.* **2004**, *38*, 4215–4221. [CrossRef]
49. Prédélus, D.; Lassabatere, L.; Coutinho, A.; Louis, C.; Brichart, T.; Slimène, E.; Winiarski, T.; Angulo-Jaramillo, R. Tracing Water Flow and Colloidal Particles Transfer in an Unsaturated Soil. *J. Water Resour. Prot.* **2014**, *6*, 696–709. [CrossRef]
50. Lin, Q.; Xu, S. Co-Transport of Heavy Metals in Layered Saturated Soil: Characteristics and Simulation. *Environ. Pollut.* **2020**, *261*, 114072. [CrossRef]
51. Jellali, S.; Diamantopoulos, E.; Kallali, H.; Bennaceur, S.; Anane, M.; Jedidi, N. Dynamic Sorption of Ammonium by Sandy Soil in Fixed Bed Columns: Evaluation of Equilibrium and Non-Equilibrium Transport Processes. *J. Environ. Manag.* **2010**, *91*, 897–905. [CrossRef]
52. Ma, J.; Wang, Y.; Stevens, G.W.; Mumford, K.A. Hydrocarbon Adsorption Performance and Regeneration Stability of Diphenyldichlorosilane Coated Zeolite and Its Application in Permeable Reactive Barriers: Column Studies. *Microporous Mesoporous Mater.* **2020**, *294*, 109843. [CrossRef]
53. Afshari, S.; Hejazi, S.H.; Kantzas, A. Longitudinal Dispersion in Heterogeneous Layered Porous Media during Stable and Unstable Pore-Scale Miscible Displacements. *Adv. Water Resour.* **2018**, *119*, 125–141. [CrossRef]
54. Afshari, S.; Hejazi, S.H.; Kantzas, A. Pore-Scale Modeling of Coupled Thermal and Solutal Dispersion in Double Diffusive-Advective Flows through Porous Media. *Int. J. Heat Mass Transf.* **2020**, *147*, 118730. [CrossRef]
55. Batany, S.; Peyneau, P.-E.; Lassabatère, L.; Béchet, B.; Faure, P.; Dangla, P. Interplay between Molecular Diffusion and Advection during Solute Transport in Macroporous Media. *Vadose Zone J.* **2019**, *18*, 1–15. [CrossRef]
56. Schlindwein, S. Parametrização Do Transporte Dispersivo de Solutos Em Solos Estruturados: Heterogeneidade Do Meio, Percurso de Transporte e Modelagem. *Rev. Bras. Ciênc. Solo* **1998**, *22*, 173–179. [CrossRef]
57. Dawodu, M.O.; Akpomie, K.G. Evaluating the Potential of a Nigerian Soil as an Adsorbent for Tartrazine Dye: Isotherm, Kinetic and Thermodynamic Studies. *Alex. Eng. J.* **2016**, *55*, 3211–3218. [CrossRef]
58. Liu, R.; Liu, X.; Tang, H.; Su, Y. Sorption Behavior of Dye Compounds onto Natural Sediment of Qinghe River. *J. Colloid Interface Sci.* **2001**, *239*, 475–482. [CrossRef]
59. Errais, E.; Duplay, J.; Elhabiri, M.; Khodja, M.; Ocampo, R.; Baltenweck-Guyot, R.; Darragi, F. Anionic RR120 Dye Adsorption onto Raw Clay: Surface Properties and Adsorption Mechanism. *Colloids Surf. Physicochem. Eng. Asp.* **2012**, *403*, 69–78. [CrossRef]
60. Lazaridis, N.K.; Keenan, H. Chitosan Beads as Barriers to the Transport of Azo Dye in Soil Column. *J. Hazard. Mater.* **2010**, *173*, 144–150. [CrossRef]
61. Defo, C.; Yerima, B.P.K.; Bemmo, N. Investigating Soils Retention Ratios and Modelling Geochemical Factors Affecting Heavy Metals Retention in Soils in a Tropical Urban Watershed. *Environ. Dev. Sustain.* **2017**, *19*, 1649–1671. [CrossRef]
62. Ben Slimene, E.; Lassabatere, L.; Šimůnek, J.; Winiarski, T.; Gourdon, R. The Role of Heterogeneous Lithology in a Glaciofluvial Deposit on Unsaturated Preferential Flow-a Numerical Study. *J. Hydrol. Hydromech.* **2017**, *65*, 209–221. [CrossRef]
63. Bien, L.B.; Predelus, D.; Lassabatere, L.; Winiarski, T.; Angulo-Jaramillo, R. Combined Effect of Infiltration, Capillary Barrier and Sloping Layered Soil on Flow and Solute Transfer in a Heterogeneous Lysimeter. *Open J. Mod. Hydrol.* **2013**, *3*, 138–153. [CrossRef]
64. Coutinho, A.P.; Lassabatere, L.; Winiarski, T.; Cabral, J.J.S.P.; Antonino, A.C.D.; Angulo-Jaramillo, R. Vadose Zone Heterogeneity Effect on Unsaturated Water Flow Modeling at Meso-Scale. *J. Water Resour. Prot.* **2015**, *7*, 353–368. [CrossRef]